# Substituent Effects in the Pyridinium Catalyzed Reduction of $CO_2$ to Methanol: Further Mechanistic Insights

Emily E. Barton Cole[a], Maor F. Baruch, Robert P. L'Esperance, Michael T. Kelly, Prasad S. Lakkaraju[b], Elizabeth L. Zeitler, and Andrew B. Bocarsly*

Frick Chemical Laboratory, Princeton University, Princeton, New Jersey 08544

[a]Present address: 11 Deerpark Dr. Suite 121, Monmouth Junction, NJ 08852

[b]Visiting Research Scientist, Princeton University. Home institution: Georgian Court University, Lakewood, NJ 08701.

*To whom correspondence should be addressed, email: bocarsly@princeton.edu

ABSTRACT

A series of substituted pyridiniums were examined for their catalytic ability to electrochemically reduce carbon dioxide to methanol. It is found that in general increased basicity of the nitrogen of the amine and higher LUMO energy of the pyridinium correlate with enhanced carbon dioxide reduction. The highest faradaic yield for methanol production at a platinum electrode was 39 ± 4% for 4-aminopyridine compared to 22 ± 2 % for pyridine . However, 4-tertbutyl and 4-dimethylamino pyridine showed decreased catalytic behavior, contrary to the enhanced activity associated with the increased basicity and LUMO energy, and suggesting that steric effects also play a significant role in the behavior of pyridinium electrocatalysts. Mechanistic models for the the reaction of the pyridinium with carbon dioxide are considered.

INTRODUCTION

The rising atmospheric level of carbon dioxide($CO_2$) is thought to be a leading factor in global climate change. [1 ] In order to address such concerns, one potential approach to reducing $CO_2$ emissions is capture and conversion of the greenhouse gas into a value-added product or fuel such as methanol. One means of $CO_2$ conversion that has been proposed is either photoelectrochemical or electrochemical reduction under aqueous conditions. Many reviews have thoroughly discussed the efforts related to electrochemical reduction of $CO_2$ to a variety of products. [2-5] Lacking from much of the work to date are catalytic conditions that allow for the efficient conversion to product at low overpotential. If an electrochemical approach is to provide a pragmatically workable solution to $CO_2$ conversion, then energy efficiency is essential. Thus, the operational potential of an industrially viable $CO_2$ to methanol cathode must be near the standard redox potential. Though few reports have shown energetically efficient conversion of $CO_2$ to methanol. [6-9] Bocarsly et al. first reported in 1994 on the low overpotential reduction of $CO_2$ to methanol at hydrogenated palladium electrodes using a homogenous pyridinium electrocatalyst. [10] Faradaic efficiencies of ~30% for methanol were achieved at overpotentials of only ~200 mV beyond the thermodynamically reversible potential of -0.52 V vs. SCE at the system pH of 5.3. The work was more recently expanded to a photoelectrochemical system utilizing a p-GaP photoelectrode which was shown to reduce $CO_2$ to methanol at a significant underpotential (300 mV) with a faradaic yield of nearly 100%. [11]

Recently, we reported on proposed mechanisms for the reduction of $CO_2$ catalyzed by the pyridinium redox couple at a platinum electrode, comparing the proposed mechanisms with available data. [12] Saveant followed our study with a similar analysis. [13] Both of these works concluded that the primary event occuring at a platinum electrode in the presence of aqueous

pyridinium is the one-electron reduction of the acid proton of pyridinium to form a surface platinum hydride intermediate. However, the two works disagreed in that the Saveant study failed to make reduced products from $CO_2$, and therefore concluded that the surface platinum hydride (in the presence of $CO_2$) only leads to hydrogen generation. This finding directly contradicts our observations, which are supported by $^{13}CO_2$ studies, that $CO_2$ is reduced to $C_1$ organics in the presence of pyridine. [10, 14] Our results using platinum electrodes are mechanistically best described by a model proposed by Batista, who has suggested that the surface platinum-hydride is the active reducing agent of a transient $CO_2$-pyridine complex. [12, 15, 16] Saveant's negative results are therefore far less compelling than our positive results.

The Batista model, invoking a $CO_2$-pyridine complex as an intermediate is expected to be dependent on the basicity of the pyridine species and perhaps on the energy of the lowest unoccupied molecular orbital (LUMO) of this species. Here, this model is examined using a group of substituted pyridinium catalysts containing various electron donating and withdrawing groups as well as groups that adjust the steric bulkiness of the nitrogen center on the heterocyclic ring. The understanding gained from this work further explores the previously proposed mechanisms, and is expected to be of utility in catalyst design for enhanced production of products from $CO_2$.

## EXPERIMENTAL

**Chemicals and materials.** All pyridine derivatives were > 98% purity and used as received without further purification (Aldrich). Either deionized or high purity water (Nanopure, Barnstead) was used to prepare the aqueous electrolyte solutions. The electrochemical system was composed of a standard two-compartment electrolysis cell to separate the cathode and anode

reactions and contained 0.5 M KCl (EMD > 99 %) as supporting electrolyte and 10 mM of the desired pyridine. The working electrode consisted of a known area Pt foil connected to a Pt wire (both Aldrich) or a Pd foil (Johnson Matthey.) Pd electrodes were hydrogenated at a current density of 15 mA $cm^{-2}$ in 1 M $H_2SO_4$ until ~ 73 C were passed. All potentials stated were referenced against a saturated calomel electrode (Accumet). The three-electrode assembly was completed with a Pt mesh electrode also connected to a Pt wire. Before and during all electrolyses, $CO_2$ (Airgas) was continuously bubbled through the electrolyte to saturate the solution. Occasionally, the continuous $CO_2$ flow was observed to remove the methanol product from the electrolysis cell. In these situations a cold trap was used to retain any vaporized product. The resulting pH of the solution was maintained at pH 4.7 to pH 5.6 depending on the substituted pyridine employed.

**Cyclic Voltammetry and Bulk Electrolyses.** Bulk electrolysis experiments were performed using a PAR 173 potentiostat-galvanostat together with a PAR 379 digital coulometer (3-electrode assembly) or a LakeShore current source (2-electrode assembly omitting the reference electrode.) Bulk electrolyses were run under galvanostatic conditions, unless otherwise noted, at 50 μA $cm^{-2}$ for 24-30 hrs. CV's were obtained using a PAR 273 potentiostat-galvanostat, or a DLK-60 electrochemical analyzer at scan rates ranging from 0.5 mV/s to 1000 mV/s at a Pt disk electrode (0.1257 $cm^2$.) The pH of the solutions were always maintained at the pH observed under $CO_2$ bubbling and were adjusted with 1 M $H_2SO_4$ under Ar.

**Gas Chromatography.** The electrolysis samples were analyzed for methanol using a gas chromatograph equipped with an FID detector. Removal of the supporting electrolyte salt was first achieved with Amberlite IRN-150 ion exchange resin (cleaned prior to use to ensure no organic artifacts by stirring in a 0.1 % v/v aqueous solution of Triton X-100 (Aldrich), filtered

and rinsed with a copious amount of water, and vacuum dried below the maximum temperature of the resin, ~60ºC) before the sample was directly injected into an HP 5890 GC which housed a DB-Wax column (Agilent Technologies.) The injector temperature was held at 200 ºC, the oven temperature maintained at 120 ºC, and the detector temperature at 200 ºC. In all cases, GC samples were controled using electrolyte samples that had not been electrochemically reduced but, were run through the ion exchange column prior to analysis.

**NMR.** NMR spectra of electrolyte volumes after bulk electrolyses were also obtained using an automated Bruker Ultrashield$^{TM}$ 500 Plus spectrometer with an excitation sculpting pulse technique for water suppression. [17] Data processing was achieved using MestReNova software. The concentrations of formate and methanol present after bulk electrolyses were determined using acetone as an internal standard.

**CV Simulations.** Simulations of experimental CV's were generated using the DigiElch 4.0 simulation software and the fitting routines and reactions described in the text. Diffusion coefficients for all species were estimated at 1 x $10^{-5}$ cm/s. The fitting routine was allowed to determine the concentration of the pyridinium form present in solution. Overall, the program determined a similar concentration as predicted by the pH of the solution. The scan rate for each experimental CV and electrode area (0.1257 $cm^2$) were imported.

**Computational Methods.** All computational calculations were performed using Gaussian 03. [18] The DFT basis set B3LYP/6-31G(D,P) was chosen since it is expected to give reasonable results for intermediate size molecules and anions. The polarizable continuum model (PCM) solvation model for water was used.

## RESULTS AND DISCUSSION

An aqueous solution saturated with $CO_2$ (~30mM at STP) and containing ~10mM of a pyridine will auto-buffer at a pH near or slightly below the pyridine's pKa. For the case of pyridine itself, (equation 1) the auto-buffer point is found to be pH=5.2.

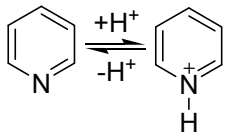


pKa = 5.2 (1)

Although, it was previously reported that the electroactive pyridinium cation can be reduced to yield the pyridinyl radical species in aqueous solution and that two of these 1e- reduced species couple to generate dihydrogen [19], recent work, as already discussed, strongly support the notion that reduction of pyridinium involves the direct reduction of the acidic proton to form $H_2$ without involvement of the ring's electronic system as outlined in equations (2 and 3).

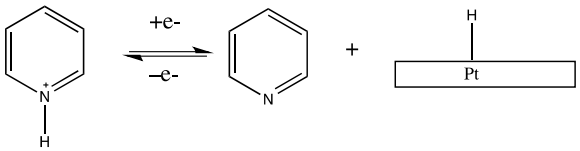


($E^o$, $k_{et}$) (2)

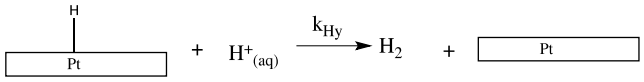


(3)

Pyridinium and the various derivatives examined in this work were studied under an argon atmosphere in aqueous electrolyte at pH adjusted using HCl(aq) to that of similar solutions saturated with $CO_2$. Figure 1 shows a comparison of experimental and simulated cyclic voltammograms (CVs) for 2-methyl pyridinium reduction and the coupled hydrogen formation reaction, following equations 1-3 above.

Table 1 summarizes these results, showing the electrochemical constants and kinetic parameters obtained from fitting the experimentally obtained CV's. The comparisons of experimental and simulated CVs for the other catalysts studied are given in the supporting information. The values in Table 1 represent average values obtained by fitting experimental

CV's over the scan rate range of 1 mV/s to 1 V/s to equations 1-3, similar to the data and digital fit shown in Figure 1. One of the compounds studied, 4-hydroxy pyridinium is omitted from the tabulated data since we propose here that the reaction mechanism for the reduction of $CO_2$ to methanol proceeds through a modified mechanism to be discussed later in this paper. The rate constants for reaction (3), which produce $H_2$ ($k_{Hy}$), were determined over a scan rate range less than or equal to 100 mV/s, which was slow enough for the simulation software to detect this step. Nicholson and Shain diagnostics correspond to the proposed EC' mechanism (equations 2-3) for pyridinium reduction and the electrocatalytic generation of hydrogen in aqueous media. The digital simulations for the set of pyridines studied here yield values for $k_{hy}$ that are similar to those obtained using a Nicholson and Shain analysis. [20, 21] We propose that this latter reaction competes with the reduction of $CO_2$ (when present) as diagrammed in scheme 1, where the relative ratio of the reaction channels is based on the observed faradaic yield of methanol when unsubstituted pyridinium is employed as the catalyst. [10, 14]

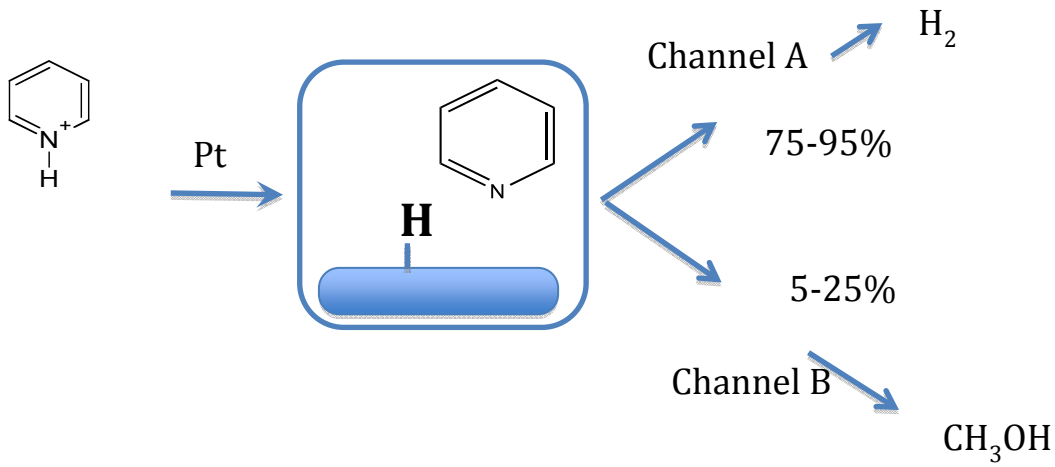


Scheme 1: Dual channel mechanism for the competitive formation of $H_2$ and methanol on a Pt-H surface. Pathway probabilities are based on the observed faradaic yield of methanol from $CO_2$.

In the pH range of 5.3-5.6 for $CO_2$-saturated solutions containing the catalysts represented in Table 1, the standard potential for the reduction of $CO_2$ to methanol ranges from -0.52 to -0.54 V vs. SCE. Cyclic voltammetric half wave analysis of all of derivatives in Table 1 have $E_R^o$s capable of reducing $CO_2$ to methanol near the thermodynamic potential for the reduction of $CO_2$ to methanol, with unsubstituted pyridine having a redox potential closest to the thermodynamic potential for $CO_2$ reduction to methanol.

The first electron-proton transfer step in the reduction of $CO_2$ to methanol has been proposed to proceed through an interaction of the platinum hydride surface with a $CO_2$-pyridine adduct, equation 4, delivering 2-electrons and a proton to $CO_2$. [15]

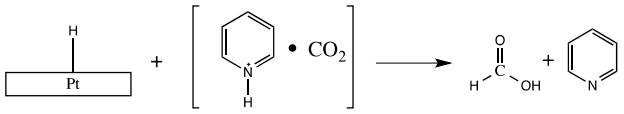


(4)

Morris et. al have reported that the overall production of methanol is first order in $CO_2$, which is consistent with the proposed mechanism. [22]

Reaction (4) replaces our earlier speculation that $CO_2$ reacted with a pyridinyl radical. The pyridinyl-based mechanism requires a nucleophilic attack by the reduced pyridinyl radical on the $CO_2$ carbon with a concomitant loss of the nitrogen proton. This however, now appears highly unlikely since the pKa for this species has been recently calculated to be ~27. [23] Thus, the nitrogen proton of pyridinyl is a non-acidic hydrogen. Therefore, any scheme that invokes a simple $S_{N1}$ mechanism in which proton loss precedes $CO_2$ attack is unlikely.

In order to further probe the mechanism of reaction of pyridinium with $CO_2$, we examined a series of pyridines with various substituent groups located at the two or four position on the pyridine ring. It was hypothesized that the basicity of the pyridine nitrogen and the LUMO ($\pi^*$) energies would both be related to pyridinium catalytic activity for $CO_2$ reduction

based on reaction (4). Figure 2 shows that there is a linear relation of the $E_R^o$'s for the pyridine series in Table 1 and pKa. This is as is expected for all weak acids where it has been shown that log(Ka) of the acid appears as a term in the Nernst equation for the reduction of the acidic proton. [12, 13] A higher pKa is associated with increased basicity, and thus, a smaller equilibrium hydronium concentration near the electrode. Separately, higher LUMO energies for the protonated aromatic entity must also correlate to more negative redox potentials for the delivered protons. The relation of the $E_R^o$s for the pyridine series in Table 1 and LUMO energies calculated using DFT methods is provided in Figure 3. Although DFT methods do not directly provide LUMO energies, it has been shown that within a homologous series LUMO energies are well approximated using this approach. [24] Figure 3 further justifies this approach since it provides a linear correlation between the calculated LUMO energy of the pyridinium catalysts and the $E_R^o$s for their 1e- reduction (Equation 2).

Table 1 lists the various catalysts studied for the catalytic electroreduction of $CO_2$ to methanol. Table 2 shows the results for constant current bulk electrolyses for the various pyridinium electrocatalysts examined. The highest faradaic yield for methanol, 39 ± 4%, was achieved using 4-amino pyridinium. In addition to methanol formation, formic acid was found to be a significant product , its concentration varying with the catalyst employed as reported in Table 2. In general, the faradaic yield for methanol and total $CO_2$-derived products were seen to increase linearly with higher LUMO energies and increased catalyst basicity, as shown in Figure 4ab. Due to the interrelation of electron density on the ring and pKa, this is expected. In this sense, the catalyst pKa can be considered the fundamental thermodynamic parameter for the reduction of aromatic amines, which is consistent with our derivation of this relationship for all week acids. [12] Herein, we show that this parameter also predicts the catalytic activity of

aromatic amines for $CO_2$ reduction. That is, referring back to Scheme 1, more basic amines enhance channel B over channel A.

Note that 4-tert-butyl pyridinium and 4-dimethylamino pyridinium, though well behaved with regard to their Nernstian response with pKa (Figure 1) and LUMO energy (Figure 2), do not follow the linear Faradaic yield trends reported in Figure 4ab. Considering the similarity of the LUMO energy and the pKa's between 4-amino and 4-dimethylamino pyridine as well as between 4-methyl and 4-tert-butyl pyridinium, a steric factor is postulated to be influential in these two cases. To further investigate the observed behavior of both the sterically hindered systems and the well behaved systems, the thermochemistry of the series of pyridinium electrocatalysts was examined by computational means. The free energies for the six proton-electron transfers in the conversion of $CO_2$ to methanol as well as the overall free energy in the production of methanol for all substituted amines examined is given in the supplemental information.

Using the total free energies for the reduction of $CO_2$ to methanol for the various substituted pyridiniums a Taft relation was examined to probe the steric effects on the pyridinium-catalyzed reduction of $CO_2$ to methanol. We have previously highlighted the possible electrode surface influence for at least two of the six electron transfers. [14] However, for this relation we are interested in the path independent, total free energies for the production of methanol from $CO_2$. Following a standard Taft relation between $\log(K_s/K_{CH3})$ (where s = -H, or $-C(CH_3)_3$) and the steric substituent constants, $E_s$, a steric sensitivity factor ($\delta$) of -0.4 was calculated, indicating the reaction rate decreases with increasing steric bulk on the pyridinium ring. Thus, these compounds follow the known reaction dynamics of sterically limited aromatic systems. It is interesting to note that the steric component is placed in the para position on the

ring. Thus, it is not inhibiting a simple interaction between $CO_2$ and the nitrogen site of the amine.

To further probe the steric effects on the pyridinium-catalyzed reduction of $CO_2$ to methanol, we examined the rate constants for three of the proposed homogenous $1e^-$ transfer steps required in the $6e^-$ reduction to methanol. These proposed mechanistic steps were the reaction of pyridinium with $CO_2$ (equation 4), the reaction of pyridinium with a formate intermediate to yield formaldehyde (equation 5), and the reaction of pyridinium with formaldehyde to yield a proposed intermediate on route to methanol (equation 6).

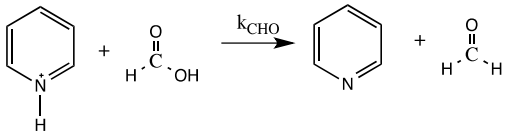


(5)

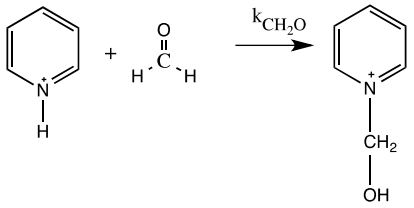


(6)

Rate constants for the three reactions (equations 4-6) were obtained by simulating experimental CVs using to the overall proposed mechanism, which involved separately obtaining and simulating cyclic voltammetric data using formic acid and formaldehyde as starting materials (in addition to $CO_2$) since these species are proposed as key intermediates and side products. Additional information on the full mechanism is given in the supporting information, including a comparison of simulated and experimental CVs for all proposed reactions.

Table 3 provides the rate constants for equations 4, 5, and 6 for the substituted pyridine catalysts examined. For 4-amino pyridine and 4-dimethylamino pyridine, rate constants were not accessible because the more negative redox potential for these species caused an overlap of their cyclic voltammetric redox processes with baseline processes (i.e. the direct reduction of $H_2O$).

The convolution of these two processes made the fitting errors too large to obtain reliable rate constants. In comparing the rate constants for these key reactions to the total faradaic yields reported in Table 2, the ratio of $k_{CO2}$ to $k_{Hy}$ was examined. A higher ratio of $k_{CO2}/k_{Hy}$ indicates a preference for reaction channel B over A (Scheme 1) and thus, a higher faradaic yield for reduced $CO_2$ products should be observed. In general the trend follows this ratio, with 2-methyl pyridine showing the highest ratio of $k_{CO2}/k_{Hy}$ and highest total faradaic yield, followed by 4-methyl pyridine, 4-tertbutyl pyridine, and pyridine. This suggests that the net rate limiting step for the complete reaction is reaction (4), which is consistent with the data reported by Morris et al. [22] Again, 4-tertbutyl pyridine proves to be an outlier in the trend, showing a higher $k_{CO2}/k_{Hy}$ ratio but lower faradaic yield for $CO_2$-derived products. This points to a different rate determining process for this compound. As noted earlier, this amine is sterically hindered, but that hindrance cannot be associated with chemistry at the nitrogen site. Therefore, we postulate that the steric constraint occurs between the aromatic amine and the platinum surface, involving either reaction (2) or (4). In either case, it may be necessary for the ring to physisorb to the electrode via a π-bonding interaction, and such an interaction might be limited by a bulky substituent in any ring position. This anomaly gives support to the complete proposed mechanism. 4-tertbutyl pyridine is a poorer performing catalyst in regards to methanol formation, however, the catalyst is ideal in selectivity for methanol over formic acid. The proposed route to formic acid involves a heterogeneous electron transfer while a surface process has not been identified at this point for the follow up reactions to generate methanol. As seen in Table 3, 4-tertbutyl pyridine has the fastest observed rate constants for equations 5-6, which are proposed to be solution processes. Thus, production of formate introduces stringent steric

requirements, but the reaction(s) of formate to generate methanol be may be solution-based process that does not have the same demanding steric requirements.

Finally, we note one other deviation from the linear response that we have observed, namely the 4-hydroxypyridine catalyst activity. This compound is well behaved both with respect to the expected Nernstian response and Faradaic yield based on pKa. However, it breaks the linear relationship found for Faradaic yield vs. LUMO. However, this species has an important resonance structure as shown in Equation (7) that makes the more acidic tautomer accessible. As a result the calculation of the LUMO based on the pure 4-hydroxy pyridine structure is not realistic. However, note as shown in Figure 4b, if the calculation is based on the quinone structure (horizontal dashed line) the linear trend observed for all of the non-sterically hindered pyridines also holds for the this system.

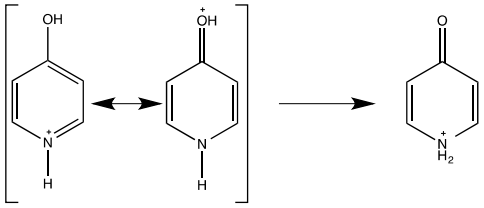


(7)

CONCLUSION

A series of substituted amines were examined for their catalytic ability to reduce $CO_2$ to methanol at Pt electrodes. Generally it appears that increased $\pi^*$ (LUMO) energy of the pyridinium and higher basicity correlates with enhanced yields of organics from $CO_2$. Compared to pyridinium, 4-amino pyridinium showed a FY increase of ~17% for methanol production. Deviations from the generalized linear response of the Faradaic yield with pKa (or LUMO) were observed when the bulkiness of the pyridinium ring was increased at the position para to the nitrogen, leading to lower Faradaic yields. For example, 4-amino and 4-dimethylamino

pyridinium have similar pKa's and LUMO energies, but generated Faradaic yields for methanol formation of ~39% and ~11% respectively. This steric effect is postulated to be associated with the ability of the amine to chemisorb to the platinum electrode surface in a π-type manner. With this further understanding of the pyridinium-catalyzed reduction of $CO_2$ to methanol, we hope to design optimized electrocatalysts for energetically efficient conversion and enhanced methanol yield.

AKNOWLEGMENTS

This work was funded by the Division of Chemical Sciences, Geosciences, and Biosciences, Office of Basic Energy Science of the U.S. Department of Energy through grant number DE-SC0002133.

## TABLES

**Table 1.** Standard potentials, kinetic constants[a], and pKa's for the electrochemical reduction of pyridinium and its analogs to generate hydrogen.

| electrocatalyst | pKa | $E^o$ (V)[b] | α | $k_s$(cm $s^{-1}$)[c] | $k_{Hy}$($M^{-1}s^{-1}$)[d] |
|---|---|---|---|---|---|
| pyridinium | 5.17 | -0.58 | 0.64 | 0.010 | $2.9_5$ |
| 2-methyl pyridinium | 5.94 | -0.64 | 0.545 | 0.0053 | 0.92 |
| 4-methyl pyridinium | 6.02 | -0.64 | 0.57 | 0.0060 | $1.3_5$ |
| 4-tertbutyl pyridinium | 6.2 | -0.62 | 0.46 | 0.0053 | 1.5 |
| 4-amino pyridinium | 9.17 | -0.79 | 0.49 | $0.0025_5$ | 16 |
| 4-dimethylamino pyridinium | 9.7 | -0.82 | 0.51 | 0.0018 | 14 |

[a]Simulations including equations 1-3, [b]All potentials referenced to the SCE, [c]Equation 2, [d]Equation 3.

**Table 2.** Results for bulk electrolyses[a] at Pt electrodes galvanostatically held at 50 μA $cm^{-2}$ for various pyridinium electrocatalysts (10 mM in 50 mL of $H_2O$ + 0.5 M KCl as supporting electrolyte, saturated with $CO_2$)

| Electro-catalyst[b] | HCOOH Faradaic Yield (%) | $CH_3OH$ Faradaic Yield (%) | Total Yield[c] (%) |
|---|---|---|---|
| 4-hydroxy pyridinium | 12 ± 1 | 15 ± 3 | 27 ± 4 |
| pyridinium | 10.8 ± 0.5 | 22 ± 2 | 33 ± 3 |
| 2-methyl pyridinium | 16 ± 4 | 26 ± 4 | 42 ± 8 |
| 4-methyl pyridinium | 7 ± 3 | 31 ± 3 | 38 ± 6 |
| 4-tertbutyl pyridinium | trace | $14._5$ ± 2 | $14._5$ ± 2 |
| 4-amino pyridinium | 12 ± 4 | 39 ± 4 | 51 ± 8 |
| 4-dimethyl amino pyridinium | 7 ± 2 | 11 ± 1 | 18 ± 3 |

[a]Represent the average over at least three experiments, [b]Formaldehyde concentrations were only detected at trace levels, [c]Total faradaic yield for observed $CO_2$-derived products.

**Table 3.**

| Electrocatalyst | $k_{CO2}$[a] ($M^{-1}s^{-1}$) | $k_{CHO}$[b] ($M^{-1}s^{-1}$) | $k_{CH2O}$[c] ($M^{-1}s^{-1}$) | $k_{CO2}/k_{Hy}$ |
|---|---|---|---|---|
| pyridinium | 1.4 | 8.9 | 23 | 0.47 |
| 2-methyl pyridinium | 13 | 4.7 | 11 | 14.1 |
| 4-methyl pyridinium | 14 | 7.6 | 33 | 10.4 |
| 4-tertbutyl pyridinium | 5.7 | 11 | 59 | 3.8 |

[a]Reaction 4, the reaction of the pyridinium with $CO_2$, [b]Reaction 5, see supporting information, the reaction of the pyridinium to yield formaldehyde, [c]Reaction 6, see supporting information, the reaction of the pyridinium with formaldehyde yielding an intermediate species on route to methanol.

**FIGURES**

**Figure 1**

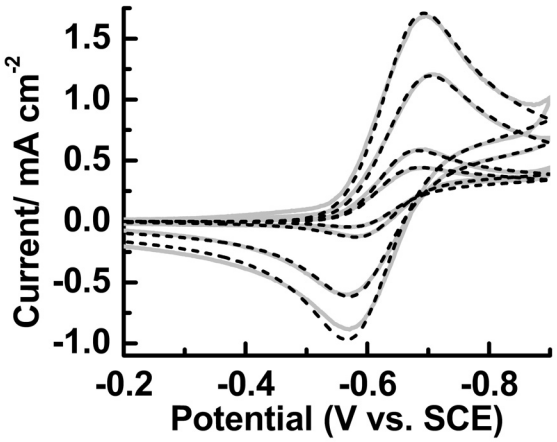


**Figure 2.**

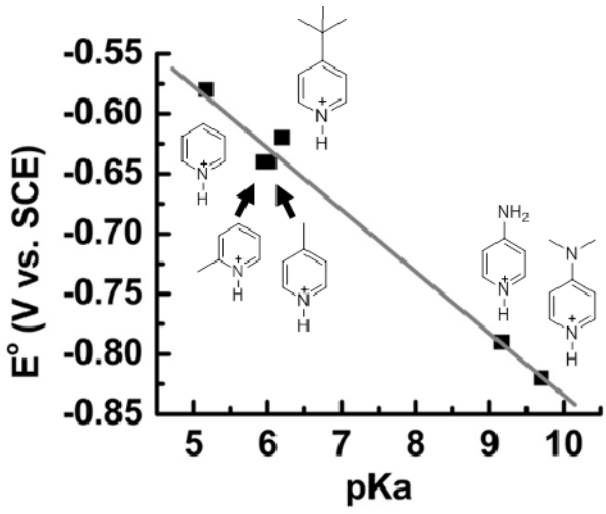

**Figure 3.**

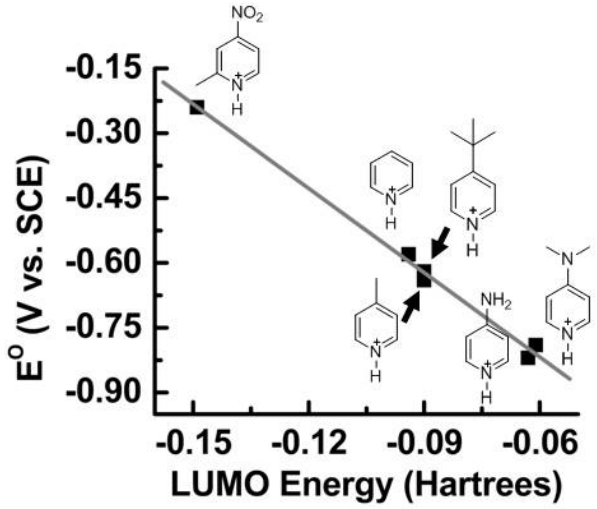


**Figure 4.**

A

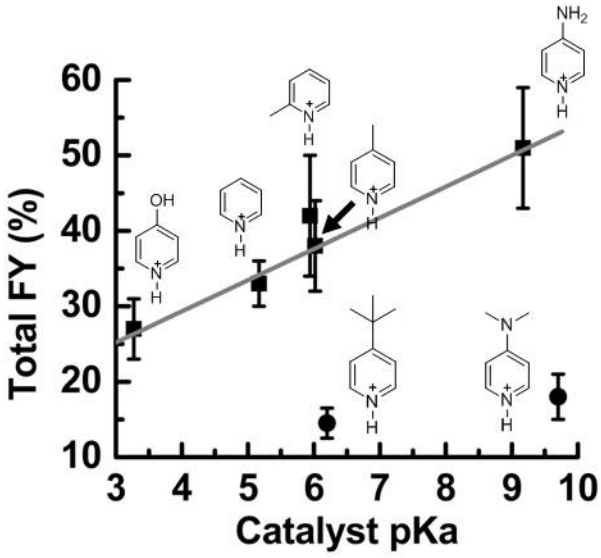


B

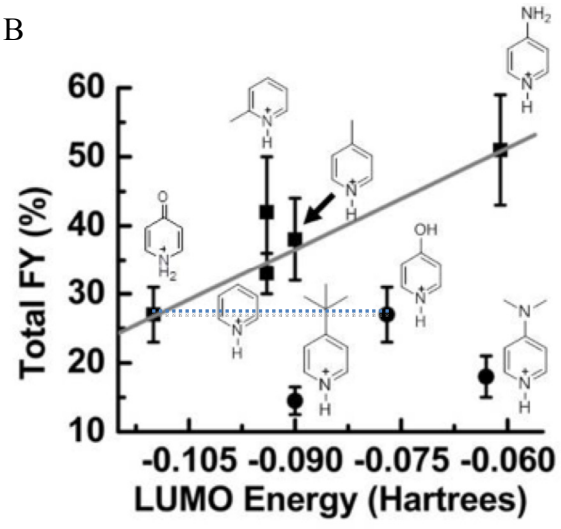

**Figure Captions**

**Figure 1.** Comparison of experimental (solid) and simulated (dash) CVs for the reduction of 2-methyl pyridinium in aqueous solution at pH 5.45 with 0.5 M KCl as supporting electrolyte. Scan rates of 5, 10, 50, and 100 mV/s are shown. The working electrode was a Pt disk (area 0.13 $cm^2$), polished using 1 μm alumina and sonicated in deionized water prior to use.

**Figure 2.** Relationship between the pKa's of the substituted pyridinium catalyst and the $E_R^o$s for the one electron reduction of each species.

**Figure 3.** Relationship between the energies of the lowest unoccupied molecular orbital's of the substituted pyridinium catalysts (LUMO) and the $E_R^o$s for the one electron reduction of each respective species.

**Figure 4**. (a) Relation between the pKa for the various substituted pyridinium catalysts and the total faradaic yield for $CO_2$-derived products. A linear increase in total faradaic yield is observed for increasing catalyst pKa. The outliers of 4-tert-butyl pyridinium and 4-dimethylamino pyridinium from the trend are attributed to steric effects. (b) Relation between the pyridine LUMO energy for the various substituted pyridinium catalysts and the total faradaic yield for $CO_2$-derived products. A linear increase in total faradaic yield is observed for less negative catalyst LUMO energy, with the exceptions noted above for steric effects. A third outlying point is found for 4-hydroxypyridine, due to the presence of the quinone form. When the LUMO energy is calculated using this tautomer (horizontal dashed line) the linear relationship is re-established.

REFERENCES


1. Coumou, D. and S. Rahmstorf, *A decade of weather extremes.* Nature Climate Change, 2012. **2**(7): p. 491-496.
2. Frese, J.K.W., *Electrochemical Reduction of CO2 at Solid Electrodes*, in *Electrochemical and Electrocatalytic Reactions of Carbon Dioxide*, B.P. Sullivan, K. Krist, and H.E. Guard, Editors. 1993, Elsevier: Amsterdam. p. 145-161.
3. Halmann, M.M. and M. Steinberg, *Electrochemical Reduction of CO2*, in *Greenhouse Gas Carbon Dioxide Mitigation: Science and Technology*, M.M. Halmann and M. Steinberg, Editors. 1999, Lewis Publishers: Boca Raton, Florida. p. 411-420.
4. DuBois, D.L., *Carbon*, in *Encylopedia of Electrochemistry*, A.J. Bard and J. Stratmann, Editors. 2006, Wiley - VCH Verlag GmbH & Co.: Weinheim, Germany. p. 202.
5. Barton-Cole, E. and A.B. Bocarsly, *Photochemical, Electrochemical, and Photoelectrochemical Reduction of Carbon Dioxide*, in *Carbon Dioxide as Chemical Feedstock*, M. Aresta, Editor. 2010, Wiley-VCH Verlag GmbH & Co.: Weinheim.
6. Bandi, A. and H.M. Kuhne, *Electrochemical Reduction of Carbon-Dioxide in Water - Analysis of Reaction-Mechanism on Ruthenium-Titanium-Oxide.* Journal of the Electrochemical Society, 1992. **139**(6): p. 1605-1610.
7. Frese, K.W. and S. Leach, *Electrochemical Reduction of Carbon-Dioxide to Methane, Methanol, and Co on Ru Electrodes.* Journal of the Electrochemical Society, 1985. **132**(1): p. 259-260.

8. Popic, J.P., M.L. AvramovIvic, and N.B. Vukovic, *Reduction of carbon dioxide on ruthenium oxide and modified ruthenium oxide electrodes in 0.5 M NaHCO3.* Journal of Electroanalytical Chemistry, 1997. **421**(1-2): p. 105-110.

9. Qu, J.P., et al., *Electrochemical reduction of CO2 on RuO2/TiO2 nanotubes composite modified Pt electrode.* Electrochimica Acta, 2005. **50**(16-17): p. 3576-3580.

10. Seshadri, G., C. Lin, and A.B. Bocarsly, *A New Homogeneous Electrocatalyst for the Reduction of Carbon-Dioxide to Methanol at Low Overpotential.* Journal of Electroanalytical Chemistry, 1994. **372**(1-2): p. 145-150.

11. Barton, E.E., D.M. Rampulla, and A.B. Bocarsly, *Selective solar-driven reduction of CO2 to methanol using a catalyzed p-GaP based photoelectrochemical cell.* Journal of the American Chemical Society, 2008. **130**(20): p. 6342-6345.

12. Yan, Y., et al., *Electrochemistry of Aqueous Pyridinium: Exploration of a Key Aspect of Electrocatalytic Reduction of CO2 to Methanol.* Journal of the American Chemical Society, 2013. **135**(38): p. 14020-14023.

13. Costentin, C., et al., *Electrochemistry of Acids on Platinum. Application to the Reduction of Carbon Dioxide in the Presence of Pyridinium Ion in Water.* J. Am. Chem. Soc., 2013. **135**(47): p. 17671–17674.

14. Cole, E.B., et al., *Using a One-Electron Shuttle for the Multielectron Reduction of CO2 to Methanol: Kinetic, Mechanistic, and Structural Insights.* Journal of the American Chemical Society, 2010. **132**(33): p. 11539-11551.

15. Ertem, M.Z., et al., *Functional Role of Pyridinium during Aqueous Electrochemical Reduction of CO2 on Pt(111).* J. Phys. Chem. Lett., 2013. **4**(5): p. 745-748.

16. Liao, K., et al., *Electrochemical Reduction of Aqueous Imidazolium on Pt (111) by Proton Coupled Electron Transfer.* Topics in Catalysis, 2014. **This Issue**: p. in press.

17. Hwang, T.L. and A.J. Shaka, *Water Suppression That Works - Excitation Sculpting Using Arbitrary Wave-Forms and Pulsed-Field Gradients.* Journal of Magnetic Resonance Series A, 1995. **112**(2): p. 275-279.

18. Inc., G., *Gaussian 03*, 2004, Gaussian Inc.: Wallingford, CT.

19. Baumgartel, H. and K.-J. Retzlav, in *Encyclopedia Of Electrochemistry Of The Elements*, A.J. Bard and H. Lund, Editors. 1984, Taylor & Francis: New York, NY. p. 194-.

20. Nicholson, R.S. and I. Shain, *Theory of Stationary Electrode Polarography - Single Scan + Cyclic Methods Applied to Reversible Irreversible + Kinetic Systems.* Analytical Chemistry, 1964. **36**(4): p. 706-723.

21. Ohmstead, M.L. and Nicholso.Rs, *Cyclic Voltammetry Theory for Disproportionation Reaction and Spherical Diffusion.* Analytical Chemistry, 1969. **41**(6): p. 862-870.

22. Morris, A.J., R.T. McGibbon, and A.B. Bocarsly, *Electrocatalytic Carbon Dioxide Activation: The Rate-Determining Step of Pyridinium-Catalyzed CO(2) Reduction.* Chemsuschem, 2011. **4**(2): p. 191-196.

23. Keith, J.A. and E.A. Carter, *Theoretical Insights into Pyridinium-Based Photoelectrocatalytic Reduction of CO2.* J. Am. Chem. Soc. , 2012. **134**(18): p. 7580-7583.

24. Zhang, G. and C.B. Musgrave, *Comparison of DFT methods for molecular orbital eigenvalue calculations.* Journal of Physical Chemistry A, 2007. **111**(8): p. 1554-1561.